



Published in final edited form as:

Br J Pharmacol. 2023 August ; 180(16): 2140–2155. doi:10.1111/bph.16071.

RGS6 negatively regulates inhibitory G protein signaling in VTA dopamine neurons and positively regulates binge-like alcohol consumption in mice

Margot C. DeBaker¹, Eric H. Mitten¹, Timothy R. Rose², Ezequiel Marron Fernandez de Velasco², Runbo Gao², Anna M. Lee², Kevin Wickman^{2,*}

¹Graduate Program in Neuroscience, University of Minnesota, Minneapolis, MN

²Department of Pharmacology, University of Minnesota, Minneapolis, MN

Abstract

Background and Purpose.—Drugs of abuse, including alcohol, increase dopamine (DA) in the mesocorticolimbic system via actions on DA neurons in the ventral tegmental area (VTA). Increased DA transmission can activate inhibitory G protein signaling pathways in VTA DA neurons, including those controlled by GABA_B (GABA_BR) and D₂ DA (D₂R) receptors. Members of the R7 subfamily of Regulator of G protein Signaling (RGS) proteins can regulate inhibitory G protein signaling, but their influence in VTA DA neurons is unclear. Here, we investigated the influence of RGS6, an R7 RGS family member that has been implicated in the regulation of alcohol consumption in mice, on inhibitory G protein signaling VTA DA neurons.

Experimental Approach.—We used molecular, electrophysiological, and genetic approaches to probe the impact of RGS6 on inhibitory G protein signaling in VTA DA neurons, and on binge-like alcohol consumption, in mice.

Key Results.—RGS6 is expressed in adult mouse VTA DA neurons and it modulates inhibitory G protein signaling in a receptor-dependent manner, tempering D₂R-induced somatodendritic currents and accelerating deactivation of synaptically evoked GABA_BR-dependent responses. *RGS6*^{-/-} mice exhibit diminished binge-like alcohol consumption, a phenotype recapitulated in female (but not male) mice lacking RGS6 selectively in VTA DA neurons.

* **Corresponding author:** Dr. Kevin Wickman, Department of Pharmacology, University of Minnesota, 312 Church Street SE, Minneapolis, MN 55455, wickm002@umn.edu, Phone: 612.624.5966.

AUTHOR CONTRIBUTIONS

Margot C. Debaker: conceptualization (supporting); data curation (lead); formal analysis (lead); investigation (lead); methodology (equal); project administration (supporting); software (equal); validation (supporting); writing-original draft (equal), writing-review and editing (supporting). **Eric H. Mitten:** investigation (supporting); data curation (supporting); formal analysis (supporting); methodology (equal); validation (supporting); writing-original draft (supporting), writing-review and editing (supporting). **Timothy R. Rose:** investigation (supporting); methodology (equal); writing-original draft (supporting), writing-review and editing (supporting). **Ezequiel Marron Fernandez de Velasco:** resources (equal), supervision (supporting); validation (equal); writing-original draft (supporting); writing-review and editing (supporting). **Runbo Gao:** data curation (supporting); formal analysis (supporting); software (equal); writing-original draft (supporting), writing-review and editing (supporting). **Anna M Lee:** funding acquisition (supporting); project administration (supporting); resources (equal), supervision (equal), writing-original draft (supporting), writing-review and editing (supporting). **Kevin Wickman:** conceptualization (lead); funding acquisition (lead); project administration (lead); resources (lead), supervision (lead); writing-original draft (equal); writing-review and editing (lead)

Competing Interest Statement The authors declare no competing interests.

Conclusions & Implications.—RGS6 negatively regulates GABA_BR- and D₂R-dependent inhibitory G protein signaling pathways in mouse VTA DA neurons and exerts a sex-dependent positive influence on binge-like alcohol consumption in adult mice. As such, RGS6 may represent a new diagnostic and/or therapeutic target for alcohol use disorder.

INTRODUCTION

The mesocorticolimbic circuitry mediates responses to natural rewards and drugs of abuse (Koob & Volkow, 2016; Uhl, Koob et al., 2019). This circuitry includes the ventral tegmental area (VTA), which projects to limbic and cortical regions that regulate distinct facets of reward processing. VTA neurons release dopamine (DA), γ -aminobutyric acid (GABA), glutamate, or combinations of neurotransmitters (Morales & Margolis, 2017). Drugs of abuse, including alcohol, enhance VTA DA neurotransmission via actions at various molecular targets (Uhl, Koob et al., 2019; You, Vandegrift et al., 2018).

VTA DA neurotransmission is negatively regulated by inhibitory G protein signaling pathways controlled by D₂ dopamine (D₂R) and GABA_B (GABA_BR) receptors (Hearing, Zink et al., 2012). For example, cocaine stimulates GABA_BR- and D₂R-dependent signaling in VTA DA neurons, tempering their excitability (Brodie & Dunwiddie, 1990; Einhorn, Johansen et al., 1988) and limiting associated drug-induced behaviors (DeBaker, Marron Fernandez de Velasco et al., 2021; Steketee & Kalivas, 1991). These pathways also shape alcohol-related behaviors (Ng & George, 1994; Vlachou & Markou, 2010). For example, mice lacking D₂R exhibit altered alcohol reward and consumption (Cunningham, Howard et al., 2000; Phillips, Brown et al., 1998), and repeated alcohol exposure enhances D₂R-dependent inhibition of VTA DA neurons (Perra, Clements et al., 2011). Furthermore, intra-VTA administration of the GABA_BR agonist baclofen reduced alcohol consumption in rodents (Maccioni, Lorrain et al., 2018; Moore & Boehm, 2009).

Regulator of G protein Signaling (RGS) proteins negatively regulate G protein signaling by enhancing the catalytic activity of G α subunits (Stewart & Fisher, 2015). R7 RGS proteins (RGS6, RGS7, RGS9, and RGS11) contain a structural module analogous to the G protein G γ subunit that promotes association with the atypical member of the G protein G β family, G β 5 (Cheever, Snyder et al., 2008); this interaction is critical to the stability and function of R7 RGS proteins (Chen, Eversole-Cire et al., 2003). R7 RGS/G β 5 complexes negatively regulate inhibitory G protein signaling in neurons (Anderson, Posokhova et al., 2009; Gerber, Squires et al., 2016) and cardiomyocytes (Posokhova, Wydeven et al., 2010; Yang, Huang et al., 2010). For example, RGS7/G β 5 sharpens the kinetics and dampens the sensitivity of GABA_BR-dependent coupling to G protein-gated inwardly rectifying K⁺ (GIRK) channels in hippocampal neurons (Ostrovskaya, Xie et al., 2014; Xie, Allen et al., 2010).

RGS6 also regulates inhibitory G protein signaling in neurons (Garzon, Lopez-Fando et al., 2003; Maity, Stewart et al., 2012; Stewart, Maity et al., 2014). Interestingly, *RGS6*^{-/-} mice exhibited decreased alcohol consumption and reward, phenotypes partially restored by systemic administration of GABA_BR or D₂R antagonists (Stewart, Maity et al., 2015). While the anatomic basis for the influence of RGS6 on alcohol consumption is unclear, voluntary

ethanol consumption increased RGS6 expression in the VTA (Stewart, Maity et al., 2015). Moreover, RGS6 expression has been detected in VTA DA neurons in both newborn and adult mice (Bifsha, Yang et al., 2014; Stewart, Maity et al., 2015). The goal of this study was to address whether inhibitory G protein signaling pathways in VTA DA neurons are regulated by RGS6 and, if so, whether this influence impacts alcohol consumption. Our findings reveal that RGS6 modulates discrete aspects of GABA_BR- and D₂R-dependent signaling in VTA DA neurons, and that loss of RGS6 in VTA DA neurons suppresses binge alcohol consumption in female but not male mice.

METHODS

Animals.

Reporting related to the animal studies in this manuscript conforms with ARRIVE guidelines (Kilkenny, Browne et al., 2010). All studies were approved by the Institutional Animal Care and Use Committee at the University of Minnesota (Protocol ID 2012–38714A). *RGS6*^{-/-} mice were generated and characterized previously (Posokhova, Wydeven et al., 2010), and kindly provided by Dr. Kirill Martemyanov. C57BL/6J mice, bred on site or purchased from The Jackson Laboratory, were used as wild-type (WT) controls for some studies. B6.SJL-*Slc6a3*^{tm1.1(cre)Bkmn}/J mice (stock #006660, The Jackson Laboratory; Bar Harbor, ME), hereafter referred to as DATCre(+) mice, were used in viral overexpression experiments. DATCre(+) mice were also crossed with a Cre-dependent Cas9GFP knock-in line (B6;129-Gt(ROSA)26Sor^{tm1(CAG-cas9*,-EGFP)}Fezh/J, The Jackson Laboratory, stock #026179), to generate DATCre(+) subjects homozygous for the Cas9GFP(+) mutation; these mice are referred to throughout as DATCre(+):Cas9GFP(+) mice and were used in all viral CRISPR/Cas9 ablation studies, as described (DeBaker, Marron Fernandez de Velasco et al., 2021). Genotypes of all mutant mice were determined using validated PCR-based protocols. All mice were group-housed; subjects involved in drinking studies were individually housed prior to assessments to monitor drinking. Mice were maintained on a 14:10 h light/dark cycle and were provided *ad libitum* access to food and water.

Reagents.

Baclofen, quinpirole, sulpiride, kynurenic acid, and picrotoxin were purchased from Sigma (St. Louis, MO), and CGP54626 was purchased from Tocris (Bristol, UK). Adeno-associated viruses (AAVs) used in this study were packaged in AAV8 serotype unless otherwise noted; the University of Minnesota Viral Vector and Cloning Core provided all but one vector used in this study, at titers ranging from 0.7–4 × 10¹³ genocopies/mL. AAV9-CaMKII α -hChR2(H134R)-mCherry was a gift from Dr. Karl Deisseroth (Addgene viral prep # 26975-AAV9), for use in *ex vivo* optogenetic experiments. Packaging plasmids (pRC8 and pHelper) were obtained from the University of Pennsylvania Vector Core. For CRISPR/Cas9 experiments, the pAAV-U6-gRNA-hSyn-NLSmCherry was generated using the backbone of the plasmid pAAV-U6-gRNA-hSyn-Cre-2A-EGFP-KASH (Platt et al., 2014) (Addgene plasmid #60231) that was a gift from Dr. Feng Zhang. Guide RNA (gRNA) sequences targeting RGS6, G α_o , and LacZ were as follows: RGS6 – TGTAGCCCTGGGCGGCAATA, G α_o – GTCGCCCCAGAGTCGCATCA, LacZ – TGCGAATACGCCACGCGAT. AAV8-hSyn-DIO-RGS6-IRES-GFP was used to

overexpress RGS6 in a Cre-dependent manner, and AAV8-hSyn-DIO-hSyn-GFP served as control vector for these studies.

In situ hybridization.

Adult (8–10 wk) C57BL/6J mice were killed by rapid decapitation following isoflurane anesthesia (induction chamber with 1 mL isoflurane); brains were removed, snap frozen in isopentane, and sectioned by cryostat (16 μ m). Sections were adhered to Superfrost[®] Plus slides, kept at -20° C for 60 min to dry, and stored at -80° C until use. Sections were fixed with 4% paraformaldehyde for 1 h and processed for multichannel fluorescent *in situ* hybridization (RNAScope) according to manufacturer instructions (Advanced Cell Diagnostics/ACD; Newark, CA). Sections were counterstained with DAPI for 20 s at room temperature, cover-slipped with Prolong Gold Antifade (ThermoFisher Scientific), and stored at 4° C. Probes for detection of DAT (NM_010020.3; target region 1486–2525), G β 5 (NM_010313.2; target region 359–1273), and RGS6 (NM_001310478.2; target region 587–1628) were purchased from ACD, and fluorescent Opal dyes (Opal 520, 620, 690) for detection of specific probes were purchased from Akoya Biosciences (Marlborough, MA). Sections containing the VTA were imaged with a BZ-X810 epifluorescent microscope (Keyence; Itasca, IL). Images for each channel were obtained from multiple focus planes and stitched using Keyence BZ-X800 analysis software; all images were acquired and processed in the same manner. Multichannel images, including DAPI, were overlaid.

Multiple (3–4) mice per group per sex were analyzed, with 2–4 images analyzed independently from each mouse. For each image, the region of interest (ROI) was selected using the Computer Vision Toolbox in MATLAB (MathWorks; Natick, MA). ROIs consisted of a consistent-sized rectangle capturing the medial and lateral VTA. ROI images were exported from MATLAB to CellProfiler 4.0 (www.cellprofiler.org) (Stirling, Swain-Bowden et al., 2021). Background fluorescence was subtracted, intensity information was removed, and images were converted to grayscale. CellProfiler was used to identify the cell area and the probe puncta within the cell. The background probe expression in areas defined as non-cell was calculated and compared with probe expression within each defined cell using MATLAB. Cells were considered positive for that probe if the puncta expression was statistically different from background expression using a binomial distribution test with a Bonferroni correction for the number of cells. The percentage of DAT-positive cells in the ROI that lacked (–) or showed (+) expression of the target of interest was determined for each independent image, and an average across images from a single animal was calculated.

Electrophysiology.

Behaviorally naïve mice (35–93 d) were killed by rapid decapitation following isoflurane anesthesia (induction chamber with 1 mL isoflurane), and acutely isolated slices (225 μ m) containing the VTA were prepared as described (DeBaker, Marron Fernandez de Velasco et al., 2021; McCall, Kotecki et al., 2017). Neurons in the lateral VTA were targeted for electrophysiological analysis as this sub-region of the VTA is enriched in neurons expressing traditional molecular (DAT) and functional (I_h and D_2R -dependent inhibition) markers of DA neurons (Lammel, Lim et al., 2014; Lammel, Steinberg et al., 2015; Morales & Margolis, 2017), and because these neurons exhibit prominent GABA β R-dependent

inhibitory feedback (Edwards, Tejada et al., 2017). In studies involving *RGS6*^{-/-} or control mice, putative DA neurons were selected based on size (apparent capacitance >40 pF), presence of an I_h current (>80 pA), and low-to-moderate rates (<5 Hz) of spontaneous activity. All command potentials factored in a junction potential of -15 mV predicted using JPCalc software (Molecular Devices, LLC).

Whole-cell data were acquired using a Multiclamp 700A amplifier and pCLAMPv.9.2 software (Molecular Devices, LLC; San Jose, CA). Input/membrane resistance (R_M) and apparent capacitance (C_M) were measured using a 5 mV/10 ms voltage-step, with current responses filtered at 5 Hz. Immediately after establishing whole-cell access, I_h was measured using a 200-ms voltage step to -120 mV; the difference in current from beginning to end of the voltage step was taken as I_h amplitude. Subsequently, spontaneous activity was measured in current-clamp mode ($I=0$) for 1 min. Neurons exhibiting no spontaneous activity were not evaluated further. For rheobase assessments, cells were held in current-clamp mode at -80 pA to prevent spontaneous activity, and then given 1-s current pulses, beginning at -100 pA and increasing in 20 pA increments. Rheobase was defined as the minimum current step that evoked one or more action potentials. Somatodendritic currents evoked by baclofen or quinpirole, applied via bath perfusion, were measured at -60 mV. Concentrations of baclofen and quinpirole evoking maximal and half-maximal current responses in VTA DA neurons, as well as concentrations of GABA_BR (CGP54626) and D₂R (sulpiride) antagonists were chosen based on prior published studies (DeBaker, Marron Fernandez de Velasco et al., 2021; McCall, Kotecki et al., 2017; McCall, Marron Fernandez de Velasco et al., 2019). Series and input resistances were tracked throughout each experiment. If series resistance was unstable or exceeded 20 MOhm, the experiment was excluded from analysis.

For optogenetic experiments, the bath solution contained kynurenic acid (2 mM) and picrotoxin (100 μ M) to block responses mediated by glutamate and GABA_A receptors, respectively. Optical stimulation was provided via a 200 μ m fiber aimed above the entire slice through a 4x objective; responses were obtained with a 1-s stimulation protocol containing 20 pulses of 473 nm wavelength light (2-5 mW, 3 ms pulse width), a protocol was shown to evoke GABA_BR-dependent inhibitory postsynaptic currents (IPSCs) in VTA DA neurons (Edwards, Tejada et al., 2017). The GABA_BR antagonist CGP54626 (2 μ M) was applied to verify the GABA_BR-dependence of optically evoked responses. Separate single-term exponential fits were assigned to the activation and deactivation phases of the optically evoked IPSCs in ClampFit (Molecular Devices, LLC; San Jose, CA).

Intracranial manipulations.

Mice (45 d) were weighed, anesthetized with a mixture of oxygen (0.5 mL/min) and isoflurane (2%) delivered via nose cone, and then placed in a stereotaxic frame using a bite bar (David Kopf Instruments; Tujunga, CA). Heads were shaved, eyes were fully covered with Artificial Tears ointment (Akorn; Gurnee, IL) applied using a sterile cotton swab, carprofen (5 mg/Kg) and gentamycin (5 mg/Kg) were administered via subcutaneous injection, and a betadine swab was used to clean the head prior to making an incision, centering and leveling the mouse skull, and drilling burr holes in the skull. Microinjectors were made by affixing a 33-gauge stainless steel hypodermic tube within a shorter 26-gauge

stainless steel hypodermic tube; injectors were attached to polyethylene-20 tubing affixed to 10 μ L Hamilton syringes, and were lowered through burr holes in the skull to the VTA (from bregma: -2.75 mm A/P, ± 0.55 mm M/L, -5 mm D/V); 400 nL of virus per side was injected at a rate of 100 nL/min. Optimized coordinates and viral load were employed to maximize coverage of the VTA along anterior/posterior and rostral-caudal axes, with minimal spread into the adjacent substantia nigra pars compacta (McCall, Kotecki et al., 2017). For neuron-specific RGS6 over-expression and ablation studies involving DATCre(+) or DATCre(+):Cas9GFP(+) mice, respectively, subjects were randomly assigned to viral treatment groups. For optogenetic slice electrophysiological experiments, microinjectors were lowered to the NAc (from bregma: $+1.7$ mm A/P, ± 1.7 M/L, -4.65 mm D/V); 400 nL of virus per side was injected at a rate of 100 nL/min. Microinjectors were left in place for 10 min following infusion to reduce solution backflow along the infusion track.

Following viral infusion, incisions were closed with sutures (3–5) and Gluture (World Precision Instruments, LLC; Sarasota, FL). Mice were removed from the stereotaxic frame and placed in a recovery cage seated on a heating pad until recovery. Ibuprofen (150 mg/500 mL) was administered via drinking water for 2 d post-surgery. Slice electrophysiology and behavioral experiments were performed 5–6 wk after viral infusion for CRISPR/Cas9 ablation experiments, and 3–4 wk after viral infusion for all other studies. Following behavioral testing, mice were killed by rapid decapitation following isoflurane anesthesia (induction chamber with 1 mL isoflurane). The scope and accuracy of viral targeting was assessed by fluorescence microscopy; 225 μ m horizontal slices of the midbrain were used for analysis of viral targeting. Only data from animals with bilateral viral-driven fluorescence, where the majority of fluorescence was confined to VTA (with minimal spread to the adjacent substantia nigra), were included in the final analysis.

Behavior.

Mice (53 d) were weighed and singly housed before the start of the drinking-in-the-dark (DID) procedure to facilitate measurement of individual intake. Unsweetened alcohol (ethanol) (Decon Labs, King of Prussia, PA) was mixed with tap water to 20% (v/v) for each experiment. The water bottle was replaced with an alcohol bottle for 2 h on Days 1 to 3, and 4 h on Day 4, beginning 2 h after the start of the dark cycle. Mice had free access to water at all other times. Ethanol consumption was measured by bottle weights before and after each drinking session. To account for bottle drippage and/or evaporation, sentinel bottles were placed in an empty mouse cage in the testing room and were weighed before and after each session. The change in sentinel bottle weight was subtracted from mouse consumption values during the session. Intake values were then calculated as amount of ethanol consumed (g) divided by mouse bodyweight (Kg).

Data and analysis.

This publication complies with all journal recommendations and requirements related to experimental design and analysis (Curtis, Alexander et al., 2018). Data are presented throughout as the mean \pm SEM. All studies were designed to yield groups of approximately equal size, balanced by sex. Statistical analysis was only undertaken for those studies where group size was at least 5. Declared group sizes for multiplex *in situ* hybridization and

behavioral data represent the number of independent values. For slice electrophysiological studies, the number of animals (N) and individual experiments (n) are provided; experiment (n) was the experimental unit used for analysis purposes. All data analysis was conducted in blind fashion, using Prism v.9 (GraphPad Software, La Jolla, CA); specific tests employed and statistical outputs are included in Table 1 and *Figure Legends*. All datasets presented in this study satisfied assumptions related to the use of parametric statistics, as assessed using the D'Agostino-Pearson test. Data points that fell outside the range of 2 standard deviations from the mean were excluded from analysis. Data were analyzed first for sex effects. Electrophysiological parameters were evaluated by 2-way ANOVA with sex and either viral treatment or genotype as factors. If a main effect of sex or an interaction between sex and viral treatment or genotype was not detected, within treatment or genotype data for male and female subjects were pooled and the combined data were analyzed by unpaired Student's t test or unpaired t test with Welch's correction if the groups had unequal variances. If a significant interaction between sex and either genotype or viral treatment was detected, and there was no significant variance in homogeneity, multiple comparisons were conducted with Sidak's *post hoc* test. Alcohol consumption during days 1–3 of the DID procedure was evaluated using 3-way ANOVA with repeated measures, with sex, genotype or viral treatment, and day as factors. Alcohol consumption during the day 4 binge session was evaluated using 2-way ANOVA, with sex and either genotype or viral treatment as factors. Differences were considered significant if $P < 0.05$.

RESULTS

Expression of RGS6 in adult mouse VTA DA neurons

We used multiplex *in situ* hybridization to determine whether RGS6 and its binding partner G β 5 are expressed in VTA DA neurons of the adult C57BL/6J mouse brain. DA neurons were identified based on expression of the dopamine transporter (DAT) (Morales & Margolis, 2017). Analysis of sections from adult male and female C57BL/6J mice revealed that G β 5 and RGS6 were expressed throughout the VTA, in both DAT-positive and DAT-negative cells (Fig. 1A,B). Consistent with prior reports (Bifsha, Yang et al., 2014; Stewart, Maity et al., 2015), G β 5 and RGS6 transcripts were detected in the vast majority (>90%) of DAT-positive cells in the adult mouse VTA (Fig. 1B).

G α_o ablation and somatodendritic inhibitory G protein signaling in VTA DA neurons

R7 RGS proteins like RGS6 exhibit a strong substrate preference for G α_o over G α_i (Hooks, Waldo et al., 2003; Masuho, Balaji et al., 2020), and as such, signaling pathways that rely on G α_o are strong candidates for regulation by RGS6. To determine whether GABA $_B$ R- and D $_2$ R-dependent signaling pathways in VTA DA neurons are potential targets of regulation by RGS6, we ablated G α_o in VTA DA neurons using a DA neuron-specific viral CRISPR/Cas9 ablation approach (DeBaker, Marron Fernandez de Velasco et al., 2021). DATCre(+):Cas9GFP(+) mice received intra-VTA infusions of AAV vectors harboring G α_o -specific or control (LacZ) guide RNA (gRNA) (Fig. 2A). Subsequently (5–6 wk later), we measured baseline neuronal excitability (spontaneous activity and rheobase), as well as D $_2$ R- and GABA $_B$ R-dependent somatodendritic currents, in VTA DA neurons (defined by GFP and mCherry fluorescence) from acutely isolated midbrain slices.

VTA DA neurons from $G\alpha_o$ gRNA-treated or LacZ gRNA-treated control mice did not differ in terms of spontaneous activity or rheobase, nor were differences detected in other physiological properties including apparent capacitance, input resistance, or I_h current amplitude (Table 1). In VTA DA neurons from mice treated with $G\alpha_o$ gRNA, however, peak somatodendritic currents evoked by the $D_{2/3}R$ agonist quinpirole were ~40% smaller than those measured in controls (Fig. 2B,C). Similarly, peak currents evoked by the $GABA_B$ R agonist baclofen were ~50% lower in VTA DA neurons from $G\alpha_o$ gRNA-treated mice relative to controls (Fig. 2B,D). We detected no main effect of sex, or interaction between sex and viral treatment, in any measured outcome. Thus, $G\alpha_o$ mediates a substantial fraction of somatodendritic D_2 R- and $GABA_B$ R-dependent signaling in VTA DA neurons from adult male and female mice.

D_2 R- and $GABA_B$ R-dependent signaling dynamics in VTA DA neurons from $RGS6^{-/-}$ mice

We next examined the impact of $RGS6$ ablation on D_2 R- and $GABA_B$ R-dependent somatodendritic currents in putative VTA DA neurons, using slices from $RGS6^{-/-}$ and wild-type mice. As we observed with $G\alpha_o$ ablation in VTA DA neurons, spontaneous activity and rheobase did not differ in VTA DA neurons from $RGS6^{-/-}$ and wild-type mice, suggesting that neither $G\alpha_o$ nor $RGS6$ regulates the baseline excitability of these neurons (Table 1). Furthermore, we observed no difference in sensitivity to baclofen (Fig. 3A,B) or in maximal baclofen-induced current amplitude (Fig. 3C) in putative VTA DA neurons from $RGS6^{-/-}$ and control mice. While there was also no difference in the sensitivity of putative VTA DA neurons from $RGS6^{-/-}$ and WT mice to quinpirole (Fig. 3D,E), two-way ANOVA of maximal quinpirole-induced currents revealed main effects of both sex and genotype (Fig. 3F); there was no interaction between sex and genotype. Loss of $RGS6$ correlated with larger maximal quinpirole currents in putative VTA DA neurons from both sexes and, consistent with our previous report (DeBaker, Marron Fernandez de Velasco et al., 2021), maximal quinpirole-induced currents in putative VTA DA neurons from females were larger than those in males, irrespective of genotype. Collectively, these data show that $RGS6$ suppresses the amplitude of D_2 R-dependent (but not $GABA_B$ R-dependent) somatodendritic currents in VTA DA neurons, but it does not impact sensitivity of VTA DA neurons to activation of either inhibitory G protein signaling pathway.

Given the dependence of $GABA_B$ R-dependent somatodendritic currents on $G\alpha_o$ (Fig. 2), the lack of impact of $RGS6$ ablation on either baclofen-induced current sensitivity (Fig. 3B) or maximal baclofen-induced current amplitude (Fig. 3C) in VTA DA neurons was surprising. R7 RGS proteins can also accelerate the kinetics of $GABA_B$ R-dependent signaling (Maity, Stewart et al., 2012; Ostrovskaya, Xie et al., 2014; Xie, Allen et al., 2010). To test whether $RGS6$ influences the kinetics of $GABA_B$ R-dependent responses in VTA DA neurons, we used an optogenetic approach with better temporal resolution to measure synaptically evoked $GABA_B$ R-dependent inhibitory postsynaptic currents (IPSCs) in VTA DA neurons, as described (Edwards, Tejeda et al., 2017). Synaptic IPSCs were reliably evoked by optogenetic stimulation of channelrhodopsin-expressing (hChR2(H134R)) NAc terminals in the VTA (Fig. 4A,B), and these currents were blocked by the $GABA_B$ R-selective antagonist CGP54626 (2 μ M; not shown). While the activation rate of optically evoked $GABA_B$ R-dependent IPSCs in putative VTA DA neurons from $RGS6^{-/-}$ mice did not differ from

controls (Fig. 4C), two-way ANOVA of deactivation rate revealed an interaction between sex and genotype. The deactivation rate of optically evoked IPSCs was significantly longer in VTA DA neurons from male and female *RGS6*^{-/-} mice, relative to wild-type counterparts. Thus, while RGS6 does not regulate the sensitivity or amplitude of GABA_BR-dependent somatodendritic currents in VTA DA neurons, it does negatively regulate the kinetics of synaptically evoked GABA_BR-dependent currents.

Bi-directional influence of RGS6 on D₂R-dependent signaling in VTA DA neurons

As constitutive *RGS6* ablation may provoke developmental adaptations that could impact or obscure roles for RGS6 in VTA DA neurons, we used the viral CRISPR/Cas9 approach to ablate RGS6 in adult VTA DA neurons. To validate the efficacy of this manipulation, we measured quinpirole sensitivity and maximal quinpirole-induced somatodendritic currents in VTA DA neurons from mice treated with control (LacZ) or RGS6 gRNA, 5–6 wk after viral treatment. We observed no difference in spontaneous activity, rheobase, or other electrophysiological parameters in VTA DA neurons from control- and RGS6 gRNA-treated mice (Table 1). Consistent with observations in VTA DA neurons from constitutive *RGS6*^{-/-} mice, RGS6 gRNA treatment did not impact quinpirole sensitivity in VTA DA neurons (Fig. 5A,B), but it did correlate with modestly larger maximal quinpirole-induced somatodendritic currents (Fig. 5C); no main effect of sex or interaction between sex and viral treatment was detected in this study.

We also used DATCre(+) mice and a Cre-dependent RGS6 expression vector to ask whether RGS6 overexpression in VTA DA neurons could suppress D₂R-dependent somatodendritic currents. Overexpression of RGS6 did not impact spontaneous activity, rheobase, or other measured parameters in VTA DA neurons from DATCre(+) mice (Table 1). Quinpirole sensitivity was comparable in VTA DA neurons from mice treated with RGS6 overexpression or control vector (Fig. 5D,E). However, two-way ANOVA analysis of maximal quinpirole-induced current amplitudes revealed main effects of sex and viral treatment, but no interaction between sex and viral treatment (Fig. 5F). These data suggest that the amplitude of D₂R-dependent somatodendritic currents in VTA DA neurons negatively correlates with the level of RGS6 expression in these neurons.

Impact of constitutive and neuron-specific RGS6 ablation on alcohol consumption

Constitutive *Rgs6*^{-/-} mice consumed less alcohol than wild-type counterparts in a 4-wk, 24-h access alcohol consumption paradigm (Stewart, Maity et al., 2015). To assess if RGS6 ablation also impacts acute binge-like alcohol consumption, we utilized a well-established “drinking-in-the-dark” (DID) model (Rhodes, Best et al., 2005; Thiele, Crabbe et al., 2014). This model mimics human binge drinking, as mice can achieve blood ethanol concentrations of 0.08 g% or higher (Crabbe, Ozburn et al., 2017), a level considered to be intoxicating for humans. Ethanol consumption was measured during drinking sessions over 4 consecutive days, with day 4 considered as the “binge” day.

We analyzed drinking in *RGS6*^{-/-} and wild-type counterparts across the first 3 days of testing using 3-way ANOVA with repeated measures. As a main effect of sex was detected ($F_{1,42}=7.62$, $P=0.0085$), we analyzed data from male and female subjects separately using

2-way ANOVA with repeated measures. Male *RGS6*^{-/-} mice drank significantly less than wild-type male counterparts; main effects of day and genotype were observed (Fig. 6A), but there was no interaction between day and genotype. Analysis of female data revealed a main effect of day, but neither a main effect of genotype nor an interaction between day and genotype was observed (Fig. 6B). Two-way ANOVA analysis of alcohol consumption during the day 4 binge session also revealed main effects of sex and genotype, but no interaction between sex and genotype (Fig. 6C). *RGS6*^{-/-} mice drank significantly less than wild-type counterparts, and females drank moderately more than males during this session, irrespective of genotype.

We next used the viral CRISPR/Cas9 ablation approach to examine the impact of VTA DA neuron-specific ablation of RGS6 on binge-like alcohol consumption in mice. Analysis by 3-way ANOVA with repeated measures revealed a main effect of sex ($F_{1,44}=7.54$, $P=0.0087$), and as such, we analyzed these data separately by sex. Two-way ANOVA with repeated measures failed to detect main effects of viral treatment during the 3 days leading up to the binge session for either males (Fig. 6D) or females (Fig. 6E). During the day 4 binge session (Fig. 6F), two-way ANOVA revealed an interaction between sex and viral treatment. While viral treatment did not impact male binge consumption, female mice treated with the RGS6 gRNA consumed significantly less alcohol than their controls. Thus, while both male and female constitutive *RGS6*^{-/-} mice exhibited reduced binge-like alcohol consumption, selective ablation of RGS6 in VTA DA neurons correlated with reduced binge-like alcohol consumption in female mice only.

DISCUSSION & CONCLUSIONS

Fisher and colleagues showed previously that *RGS6*^{-/-} mice exhibit diminished voluntary alcohol consumption and that systemic administration of GABA_BR or D₂R antagonists partially rescued this deficit (Stewart, Maity et al., 2015). While the pharmacologic rescue suggests that enhancement of GABA_BR- and D₂R-dependent signaling contributes to the reduced alcohol consumption, the anatomic and cellular basis of these findings are unclear. Here, we show that RGS6 is expressed in VTA DA neurons of the adult mouse and that it negatively regulates discrete aspects of D₂R and GABA_BR-dependent somatodendritic signaling pathways. Furthermore, we report that binge-like alcohol consumption is also suppressed in constitutive *RGS6*^{-/-} mice, and this deficit is recapitulated in female mice following selective ablation of RGS6 in VTA DA neurons.

R7 RGS proteins exhibit a strong substrate specificity for Gα_o relative to Gα_i (Hooks, Waldo et al., 2003; Masuho, Balaji et al., 2020), and this prompted our interest in Gα_o and its potential contribution to inhibitory G protein signaling in VTA DA neurons. While signaling preferences for discrete Gα isoforms have not been defined systematically for GABA_BR, D₂R can signal effectively through Gα_o, Gα_i and Gα_z isoforms, with the greatest responses elicited via Gα_o (Hauser, Avet et al., 2022; Masuho, Ostrovskaya et al., 2015; Von Moo, Harpoe et al., 2022). Our efforts show that Gα_o is a prominent mediator of somatodendritic GABA_BR- and D₂R-dependent signaling in VTA DA neurons of the adult mouse. Indeed, the amplitude of currents evoked by activation of either receptor was reduced by 40–50% in VTA DA neurons from adult mice treated with the Gα_o gRNA. The residual

D₂R- and GABA_BR-dependent currents seen following Gα_o ablation might indicate that a significant proportion of inhibitory signaling regulator by these receptors is mediated by Gα_i and thus not subject to strong modulation by R7 RGS proteins. It is also possible that under normal conditions these receptors preferentially engage Gα_o, but that in the absence of Gα_o they compensate by recruiting one or more Gα_i isoforms.

Constitutive ablation of RGS6 correlated with increased amplitude of D₂R-dependent somatodendritic currents, an effect recapitulated with VTA DA neuron-specific RGS6 ablation. Moreover, RGS6 overexpression suppressed the amplitude of D₂R-dependent currents in VTA DA neurons, showing that the amplitude of D₂R-dependent somatodendritic currents in VTA DA neurons can be bi-directionally regulated by RGS6. In contrast, RGS6 ablation had no impact on the amplitude of GABA_BR-dependent somatodendritic currents. Instead, RGS6 ablation prolonged the deactivation rate of evoked GABA_BR-dependent IPSCs in VTA DA neurons. These outcomes are reminiscent of findings from our recent study in sinoatrial nodal (SAN) cells (Anderson, Masuho et al., 2020); the amplitude of A₁ adenosine receptor-induced currents was greater in SAN cells from *RGS6*^{-/-} mice as compared to wild-type controls, while only the deactivation rate of M₂ muscarinic receptor-mediated currents was impacted by RGS6 ablation. Thus, RGS6 can negatively regulate inhibitory G protein signaling in neurons and cardiomyocytes, but the nature of the regulation is dependent upon the GPCR.

The GPCR-dependent influence of RGS6 on inhibitory signaling could reflect differences in the relative stoichiometries of key signaling elements found within a particular cell type. For example, GABA_BR-dependent signaling in VTA DA neurons may be limited by effector availability, whereas D₂R-dependent signaling may be limited by receptor availability. While the inhibitory effect of D₂R and GABA_BR activation in VTA DA neurons is mediated by multiple somatodendritic effectors (Labouebe, Lomazzi et al., 2007; Philippart & Khaliq, 2018), most (>80%) of the current measured under the conditions employed in this study reflect the activation of G protein-gated inwardly rectifying K⁺ (GIRK/Kir3) channels formed by GIRK2 and GIRK3 (Cruz, Ivanova et al., 2004; Labouebe, Lomazzi et al., 2007). Loss of RGS6 (and its catalytic influence on GTP hydrolysis) should increase the pool of activated G proteins following receptor stimulation. If the strength of D₂R-dependent signaling in VTA DA neurons is limited by D₂R availability, increasing the pool of activated G proteins should yield larger D₂R-induced currents. In contrast, if the strength of GABA_BR-dependent signaling in VTA DA neurons is limited by the effector (GIRK channel), then increasing the pool of activated G proteins should not impact the amplitude of the GABA_BR-induced current but it should prolong the deactivation kinetics. Consistent with this overall premise, viral over-expression of GIRK2 in VTA DA neurons increased the maximal amplitude of GABA_BR-dependent somatodendritic currents but did not significantly increase the amplitude of D₂R-dependent currents (McCall, Marron Fernandez de Velasco et al., 2019).

Consistent with our previous report (DeBaker, Marron Fernandez de Velasco et al., 2021), we observed moderately larger D₂R-induced somatodendritic current amplitudes in VTA DA neurons from female mice as compared to males (Fig. 3F). This relatively modest sex difference was evident in our analysis of maximal quinpirole-induced currents in VTA

DA neurons from *RGS6*^{-/-} mice and wild-type controls, and in our RGS6 over-expression study involving DATCre(+) mice (Fig. 5F), but it was not seen in our study involving DATCre(+):Cas9GFP(+) mice and the CRISPR/Cas9-mediated ablation of RGS6 (Fig. 5C). This discrepancy could reflect subtle changes in genetic background across the various strains used in this project. The substantial cell-to-cell variability in D₂R expression levels across the heterogeneous population of VTA DA neurons in the mouse (Morales & Margolis, 2017), combined with the relatively unguided process for selecting cells for slice electrophysiological analysis, could also collaborate to mask a small but significant sex effect such as this.

Intra-VTA infusions of baclofen decreased binge alcohol consumption in mice (Moore & Boehm, 2009), and systemic injections of the D₂R agonist quinpirole decreased alcohol sensitivity (Cohen, Perrault et al., 1997). While these studies lack cellular and/or anatomic specificity, a growing body of evidence suggests that inhibitory G protein signaling in VTA DA neurons shapes behavioral responses to drugs of abuse in rodents. For example, chemogenetic (hM4Di) inhibition of VTA DA neurons suppressed the motor stimulatory effect of cocaine and morphine in mice (DeBaker, Marron Fernandez de Velasco et al., 2021). Chemogenetic inhibition of VTA DA neurons has also been shown to reduce conditioned stimulus-induced alcohol seeking behavior (Valyear, Glovaci et al., 2020), and suppressed relapse to alcohol-seeking behavior (Liu, Jean-Richard-Dit-Bressel et al., 2020). Our results suggest that loss of RGS6, and the corresponding enhancement of VTA DA neuron D₂R- and/or GABA_BR-dependent signaling, contributes to the decrease in alcohol consumption seen in both chronic and binge voluntary consumption models, at least in female mice.

Male and female *RGS6*^{-/-} mice showed decreased binge alcohol consumption. We also observed a main effect of sex, consistent with previous reports that female rodents consume more alcohol than males (Cunningham & Shields, 2018; Li & Lumeng, 1984; Yoneyama, Crabbe et al., 2008). The deficit in binge alcohol consumption seen in constitutive *RGS6*^{-/-} mice was recapitulated in female (but not male) mice lacking RGS6 in VTA DA neurons. This finding could suggest that the binge drinking deficit noted in constitutive male *RGS6*^{-/-} mice is unrelated to the influence of RGS6 on inhibitory G protein signaling in VTA DA neurons. The differential behavioral impact of RGS6 ablation in male and female mice could be linked to the higher proportion of VTA DA neurons seen in female rodents as compared to males (McArthur, McHale et al., 2007). All else being equal in this case, manipulations of VTA DA neurons would be expected to exert a greater influence on behavior in female mice as compared to males. Finally, RGS6 may exert a stronger influence on key aspects of inhibitory G protein signaling in VTA DA neurons from female mice as compared to males. In support of this contention, VTA DA neurons from female mice lacking RGS6 showed a more prolonged deactivation of optically evoked GABA_BR-dependent IPSCs as compared to neurons from male mice lacking RGS6 (Fig. 4D).

In sum, we report here that loss of RGS6 in VTA DA neurons enhances inhibitory G protein signaling and decreases alcohol consumption, the latter in a sex-dependent manner. These data shed new light on the cellular and molecular mechanisms that regulate alcohol consumption and reward. The knowledge gained about RGS6 involvement in alcohol

consumption may guide the identification of potential risk factors associated with AUD, as a quantitative trait single nucleotide polymorphism in RGS6 was significantly associated with alcohol dependence symptom count in a human Genome Wide Association Study (Chen, Zhang et al., 2017). In addition, insights from these studies could inform investigations into new or improved therapeutic strategies for more targeted treatment of AUD.

ACKNOWLEDGEMENTS

The authors would like to thank Courtney Wright, Fayzeh El Banna, and Shaydel Engel for exceptional care of the mouse colony, and Dr. Kirill Martemyanov for providing helpful comments on the manuscript. This work was supported by NIH grants to MCD (AA028726), EHM and TRR (DA007234), AML (AA026598), and KW (DA034696, AA027544).

Declaration

This Declaration acknowledges that this paper adheres to the principles for transparent reporting and scientific rigour of preclinical research as stated in BJP guidelines for Design and Analysis and Animal Experimentation, and as recommended by funding agencies, publishers and other organizations engaged with supporting research.

Data Availability Statement

The data that support the findings of this study are available from the corresponding author upon reasonable request.

Non-standard abbreviations

AAV	adeno-associated virus
D₂R	D ₂ dopamine receptor
DA	dopamine
DAT	dopamine transporter
DID	drinking-in-the-dark
GABA	gamma aminobutyric acid
GABA_BR	GABA _B receptor
GIRK channel	G protein-gated inwardly rectifying K ⁺ channel
NAc	nucleus accumbens
RGS	Regulator of G protein Signaling
VTA	ventral tegmental area

REFERENCES

- Anderson A, Masuho I, Marron Fernandez de Velasco E, Nakano A, Birnbaumer L, Martemyanov KA, & Wickman K (2020). GPCR-dependent biasing of GIRK channel signaling dynamics by RGS6 in mouse sinoatrial nodal cells. *Proc Natl Acad Sci U S A* 117: 14522–14531. [PubMed: 32513692]
- Anderson GR, Posokhova E, & Martemyanov KA (2009). The R7 RGS protein family: multi-subunit regulators of neuronal G protein signaling. *Cell Biochem Biophys* 54: 33–46. [PubMed: 19521673]

- Bifsha P, Yang J, Fisher RA, & Drouin J (2014). Rgs6 is required for adult maintenance of dopaminergic neurons in the ventral substantia nigra. *PLoS Genet* 10: e1004863. [PubMed: 25501001]
- Brodie MS, & Dunwiddie TV (1990). Cocaine effects in the ventral tegmental area: evidence for an indirect dopaminergic mechanism of action. *Naunyn Schmiedebergs Arch Pharmacol* 342: 660–665. [PubMed: 2096297]
- Cheever ML, Snyder JT, Gershburg S, Siderovski DP, Harden TK, & Sondek J (2008). Crystal structure of the multifunctional Gbeta5-RGS9 complex. *Nat Struct Mol Biol* 15: 155–162. [PubMed: 18204463]
- Chen CK, Eversole-Cire P, Zhang H, Mancino V, Chen YJ, He W, Wensel TG, & Simon MI (2003). Instability of GGL domain-containing RGS proteins in mice lacking the G protein beta-subunit Gbeta5. *Proc Natl Acad Sci U S A* 100: 6604–6609. [PubMed: 12738888]
- Chen G, Zhang F, Xue W, Wu R, Xu H, Wang K, & Zhu J (2017). An association study revealed substantial effects of dominance, epistasis and substance dependence co-morbidity on alcohol dependence symptom count. *Addict Biol* 22: 1475–1485. [PubMed: 27151647]
- Cohen C, Perrault G, & Sanger DJ (1997). Evidence for the involvement of dopamine receptors in ethanol-induced hyperactivity in mice. *Neuropharmacology* 36: 1099–1108. [PubMed: 9294975]
- Crabbe JC, Ozburn AR, Metten P, Barkley-Levenson A, Schlumbohm JP, Spence SE, Hack WR, & Huang LC (2017). High Drinking in the Dark (HDID) mice are sensitive to the effects of some clinically relevant drugs to reduce binge-like drinking. *Pharmacol Biochem Behav* 160: 55–62. [PubMed: 28827047]
- Cruz HG, Ivanova T, Lunn ML, Stoffel M, Slesinger PA, & Lüscher C (2004). Bi-directional effects of GABA(B) receptor agonists on the mesolimbic dopamine system. *Nat Neurosci* 7: 153–159. [PubMed: 14745451]
- Cunningham CL, Howard MA, Gill SJ, Rubinstein M, Low MJ, & Grandy DK (2000). Ethanol-conditioned place preference is reduced in dopamine D2 receptor-deficient mice. *Pharmacol Biochem Behav* 67: 693–699. [PubMed: 11166059]
- Cunningham CL, & Shields CN (2018). Effects of sex on ethanol conditioned place preference, activity and variability in C57BL/6J and DBA/2J mice. *Pharmacol Biochem Behav* 173: 84–89. [PubMed: 30036544]
- Curtis MJ, Alexander S, Cirino G, Docherty JR, George CH, Giembycz MA, Hoyer D, Insel PA, Izzo AA, Ji Y, MacEwan DJ, Sobey CG, Stanford SC, Teixeira MM, Wonnacott S, & Ahluwalia A (2018). Experimental design and analysis and their reporting II: updated and simplified guidance for authors and peer reviewers. *Br J Pharmacol* 175: 987–993. [PubMed: 29520785]
- DeBaker MC, Marron Fernandez de Velasco E, McCall NM, Lee AM, & Wickman K (2021). Differential Impact of Inhibitory G-Protein Signaling Pathways in Ventral Tegmental Area Dopamine Neurons on Behavioral Sensitivity to Cocaine and Morphine. *Eneuro* 8:ENEURO.0081–21.2021.
- Edwards NJ, Tejada HA, Pignatelli M, Zhang S, McDevitt RA, Wu J, Bass CE, Bettler B, Morales M, & Bonci A (2017). Circuit specificity in the inhibitory architecture of the VTA regulates cocaine-induced behavior. *Nat Neurosci* 20: 438–448. [PubMed: 28114294]
- Einhorn LC, Johansen PA, & White FJ (1988). Electrophysiological effects of cocaine in the mesoaccumbens dopamine system: studies in the ventral tegmental area. *J Neurosci* 8: 100–112. [PubMed: 3339402]
- Garzon J, Lopez-Fando A, & Sanchez-Blazquez P (2003). The R7 subfamily of RGS proteins assists tachyphylaxis and acute tolerance at mu-opioid receptors. *Neuropsychopharmacology* 28: 1983–1990. [PubMed: 12902995]
- Gerber KJ, Squires KE, & Hepler JR (2016). Roles for Regulator of G Protein Signaling Proteins in Synaptic Signaling and Plasticity. *Mol Pharmacol* 89: 273–286. [PubMed: 26655302]
- Hauser AS, Avet C, Normand C, Mancini A, Inoue A, Bouvier M, & Gloriam DE (2022). Common coupling map advances GPCR-G protein selectivity. *Elife* 11:e74107. [PubMed: 35302494]
- Hearing MC, Zink AN, & Wickman K (2012). Cocaine-induced adaptations in metabotropic inhibitory signaling in the mesocorticolimbic system. *Rev Neurosci* 23: 325–351. [PubMed: 22944653]

- Hooks SB, Waldo GL, Corbitt J, Bodor ET, Krumins AM, & Harden TK (2003). RGS6, RGS7, RGS9, and RGS11 stimulate GTPase activity of Gi family G-proteins with differential selectivity and maximal activity. *J Biol Chem* 278: 10087–10093. [PubMed: 12531899]
- Kilkenny C, Browne W, Cuthill IC, Emerson M, Altman DG, & Group N. C. R. R. G. W. (2010). Animal research: reporting in vivo experiments: the ARRIVE guidelines. *Br J Pharmacol* 160: 1577–1579. [PubMed: 20649561]
- Koob GF, & Volkow ND (2016). Neurobiology of addiction: a neurocircuitry analysis. *Lancet Psychiatry* 3: 760–773. [PubMed: 27475769]
- Labouebe G, Lomazzi M, Cruz HG, Creton C, Lujan R, Li M, Yanagawa Y, Obata K, Watanabe M, Wickman K, Boyer SB, Slesinger PA, & Luscher C (2007). RGS2 modulates coupling between GABAB receptors and GIRK channels in dopamine neurons of the ventral tegmental area. *Nat Neurosci* 10: 1559–1568. [PubMed: 17965710]
- Lammel S, Lim BK, & Malenka RC (2014). Reward and aversion in a heterogeneous midbrain dopamine system. *Neuropharmacology* 76: 351–359. [PubMed: 23578393]
- Lammel S, Steinberg EE, Foldy C, Wall NR, Beier K, Luo L, & Malenka RC (2015). Diversity of transgenic mouse models for selective targeting of midbrain dopamine neurons. *Neuron* 85: 429–438. [PubMed: 25611513]
- Li TK, & Lumeng L (1984). Alcohol preference and voluntary alcohol intakes of inbred rat strains and the National Institutes of Health heterogeneous stock of rats. *Alcohol Clin Exp Res* 8: 485–486. [PubMed: 6391261]
- Liu Y, Jean-Richard-Dit-Bressel P, Yau JO, Willing A, Prasad AA, Power JM, Killcross S, Clifford CWG, & McNally GP (2020). The Mesolimbic Dopamine Activity Signatures of Relapse to Alcohol-Seeking. *J Neurosci* 40: 6409–6427. [PubMed: 32669355]
- Maccioni P, Lorrain I, Contini A, Leite-Morris K, & Colombo G (2018). Microinjection of baclofen and CGP7930 into the ventral tegmental area suppresses alcohol self-administration in alcohol-preferring rats. *Neuropharmacology* 136: 146–158. [PubMed: 29050951]
- Maity B, Stewart A, Yang J, Loo L, Sheff D, Shepherd AJ, Mohapatra DP, & Fisher RA (2012). Regulator of G protein signaling 6 (RGS6) protein ensures coordination of motor movement by modulating GABAB receptor signaling. *J Biol Chem* 287: 4972–4981. [PubMed: 22179605]
- Masuho I, Balaji S, Muntean BS, Skamangas NK, Chavali S, Tesmer JGG, Babu MM, & Martemyanov KA (2020). A Global Map of G Protein Signaling Regulation by RGS Proteins. *Cell* 183: 503–521 e519. [PubMed: 33007266]
- Masuho I, Ostrovskaya O, Kramer GM, Jones CD, Xie K, & Martemyanov KA (2015). Distinct profiles of functional discrimination among G proteins determine the actions of G protein-coupled receptors. *Sci Signal* 8: ra123.
- McArthur S, McHale E, & Gillies GE (2007). The size and distribution of midbrain dopaminergic populations are permanently altered by perinatal glucocorticoid exposure in a sex- region- and time-specific manner. *Neuropsychopharmacology* 32: 1462–1476. [PubMed: 17164817]
- McCall NM, Kotecki L, Dominguez-Lopez S, Marron Fernandez de Velasco E, Carlblom N, Sharpe AL, Beckstead MJ, & Wickman K (2017). Selective Ablation of GIRK Channels in Dopamine Neurons Alters Behavioral Effects of Cocaine in Mice. *Neuropsychopharmacology* 42: 707–715. [PubMed: 27468917]
- McCall NM, Marron Fernandez de Velasco E, & Wickman K (2019). GIRK Channel Activity in Dopamine Neurons of the Ventral Tegmental Area Bidirectionally Regulates Behavioral Sensitivity to Cocaine. *J Neurosci* 39: 3600–3610. [PubMed: 30837265]
- Moore EM, & Boehm SL 2nd, (2009). Site-specific microinjection of baclofen into the anterior ventral tegmental area reduces binge-like ethanol intake in male C57BL/6J mice. *Behav Neurosci* 123: 555–563. [PubMed: 19485562]
- Morales M, & Margolis EB (2017). Ventral tegmental area: cellular heterogeneity, connectivity and behaviour. *Nat Rev Neurosci* 18: 73–85. [PubMed: 28053327]
- Ng GY, & George SR (1994). Dopamine receptor agonist reduces ethanol self-administration in the ethanol-preferring C57BL/6J inbred mouse. *Eur J Pharmacol* 269: 365–374. [PubMed: 7895775]

- Ostrovskaya O, Xie K, Masuho I, Fajardo-Serrano A, Lujan R, Wickman K, & Martemyanov KA (2014). RGS7/Gbeta5/R7BP complex regulates synaptic plasticity and memory by modulating hippocampal GABABR-GIRK signaling. *Elife* 3: e02053. [PubMed: 24755289]
- Perra S, Clements MA, Bernier BE, & Morikawa H (2011). In Vivo Ethanol Experience Increases D(2) Autoinhibition in the Ventral Tegmental Area. *Neuropsychopharmacology* 36: 993–1002. [PubMed: 21248720]
- Philippart F, & Khaliq ZM (2018). Gi/o protein-coupled receptors in dopamine neurons inhibit the sodium leak channel NALCN. *Elife* 7:e40984. [PubMed: 30556810]
- Phillips TJ, Brown KJ, Burkhart-Kasch S, Wenger CD, Kelly MA, Rubinstein M, Grandy DK, & Low MJ (1998). Alcohol preference and sensitivity are markedly reduced in mice lacking dopamine D2 receptors. *Nat Neurosci* 1: 610–615. [PubMed: 10196569]
- Posokhova E, Wydeven N, Allen KL, Wickman K, & Martemyanov KA (2010). RGS6/Gbeta5 complex accelerates IKACH gating kinetics in atrial myocytes and modulates parasympathetic regulation of heart rate. *Circ Res* 107: 1350–1354. [PubMed: 20884879]
- Rhodes JS, Best K, Belknap JK, Finn DA, & Crabbe JC (2005). Evaluation of a simple model of ethanol drinking to intoxication in C57BL/6J mice. *Physiol Behav* 84: 53–63. [PubMed: 15642607]
- Steketee JD, & Kalivas PW (1991). Sensitization to psychostimulants and stress after injection of pertussis toxin into the A10 dopamine region. *J Pharmacol Exp Ther* 259: 916–924. [PubMed: 1941636]
- Stewart A, & Fisher RA (2015). Introduction: G Protein-coupled Receptors and RGS Proteins. *Prog Mol Biol Transl Sci* 133: 1–11. [PubMed: 26123299]
- Stewart A, Maity B, Anderegg SP, Allamargot C, Yang J, & Fisher RA (2015). Regulator of G protein signaling 6 is a critical mediator of both reward-related behavioral and pathological responses to alcohol. *Proc Natl Acad Sci U S A* 112: E786–795. [PubMed: 25646431]
- Stewart A, Maity B, Wunsch AM, Meng F, Wu Q, Wemmie JA, & Fisher RA (2014). Regulator of G-protein signaling 6 (RGS6) promotes anxiety and depression by attenuating serotonin-mediated activation of the 5-HT(1A) receptor-adenylyl cyclase axis. *FASEB J* 28: 1735–1744. [PubMed: 24421401]
- Stirling DR, Swain-Bowden MJ, Lucas AM, Carpenter AE, Cimini BA, & Goodman A (2021). CellProfiler 4: improvements in speed, utility and usability. *BMC Bioinformatics* 22: 433. [PubMed: 34507520]
- Thiele TE, Crabbe JC, & Boehm SL 2nd, (2014). “Drinking in the Dark” (DID): a simple mouse model of binge-like alcohol intake. *Curr Protoc Neurosci* 68: 9 49 41–12.
- Uhl GR, Koob GF, & Cable J (2019). The neurobiology of addiction. *Ann N Y Acad Sci* 1451: 5–28. [PubMed: 30644552]
- Valyear MD, Glovaci I, Zaari A, Lahlou S, Trujillo-Pisanty I, Andrew Chapman C, & Chaudhri N (2020). Dissociable mesolimbic dopamine circuits control responding triggered by alcohol-predictive discrete cues and contexts. *Nat Commun* 11: 3764. [PubMed: 32724058]
- Vlachou S, & Markou A (2010). GABAB receptors in reward processes. *Adv Pharmacol* 58: 315–371. [PubMed: 20655488]
- Von Moo E, Harpsoe K, Hauser AS, Masuho I, Brauner-Osborne H, Gloriam DE, & Martemyanov KA (2022). Ligand-directed bias of G protein signaling at the dopamine D2 receptor. *Cell Chem Biol* 29: 226–238 e224. [PubMed: 34302750]
- Xie K, Allen KL, Kourrich S, Colon-Saez J, Thomas MJ, Wickman K, & Martemyanov KA (2010). Gbeta5 recruits R7 RGS proteins to GIRK channels to regulate the timing of neuronal inhibitory signaling. *Nat Neurosci* 13: 661–663. [PubMed: 20453851]
- Yang J, Huang J, Maity B, Gao Z, Lorca RA, Gudmundsson H, Li J, Stewart A, Swaminathan PD, Ibeawuchi SR, Shepherd A, Chen CK, Kutschke W, Mohler PJ, Mohapatra DP, Anderson ME, & Fisher RA (2010). RGS6, a modulator of parasympathetic activation in heart. *Circ Research* 107: 1345–1349.
- Yoneyama N, Crabbe JC, Ford MM, Murillo A, & Finn DA (2008). Voluntary ethanol consumption in 22 inbred mouse strains. *Alcohol* 42: 149–160. [PubMed: 18358676]

You C, Vandegrift B, & Brodie MS (2018). Ethanol actions on the ventral tegmental area: novel potential targets on reward pathway neurons. *Psychopharmacology (Berl)* 235: 1711–1726. [PubMed: 29549390]

Author Manuscript

Author Manuscript

Author Manuscript

Author Manuscript

BULLET POINT SUMMARY**What is already known**

- D₂R and GABA_BR signaling pathways regulate VTA DA neuron excitability and alcohol-related behaviors
- R7 RGS proteins like RGS6 negatively regulate inhibitory G protein signaling

What this study adds

- RGS6 negatively regulates GABA_BR and D₂R-dependent signaling in VTA DA neurons in discrete manners
- RGS6 ablation in VTA DA neurons promotes increased binge-like alcohol consumption in female mice

Clinical significance

- RGS6 may represent a new diagnostic and/or therapeutic target for alcohol use disorder

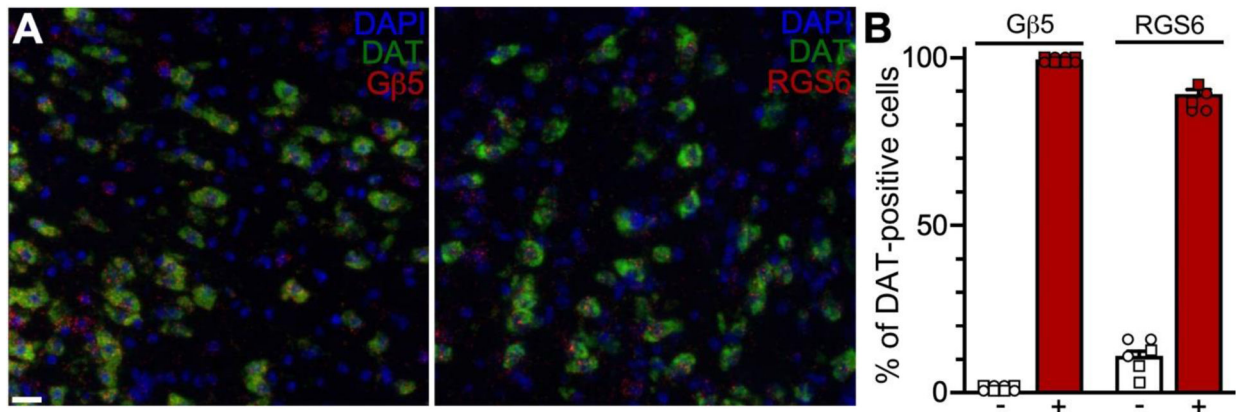


Figure 1. RGS6 and Gβ5 are expressed in VTA DA neurons of the adult C57BL/6J mouse

A. Representative images from multiplex *in situ* hybridization experiments showing expression of Gβ5 (red; left panel) or RGS6 (red; right panel) in cells of the adult C57BL/6J mouse VTA. DAT expression is indicated in green and DAPI labeling is shown in blue. Scale bar: 20 μm.

B. Summary of coded analysis of images from the multiplex *in situ* hybridization experiments. Expression of each target in the VTA was evaluated in 3–4 mice per sex. The percentage of DAT-positive cells that lacked (–) or showed (+) expression of the target of interest was determined for each subject; squares and circles denote datapoints from male and female subjects, respectively. Approximately 99% of DAT-positive cells express Gβ5 and 90% of DAT-positive cells express RGS6.

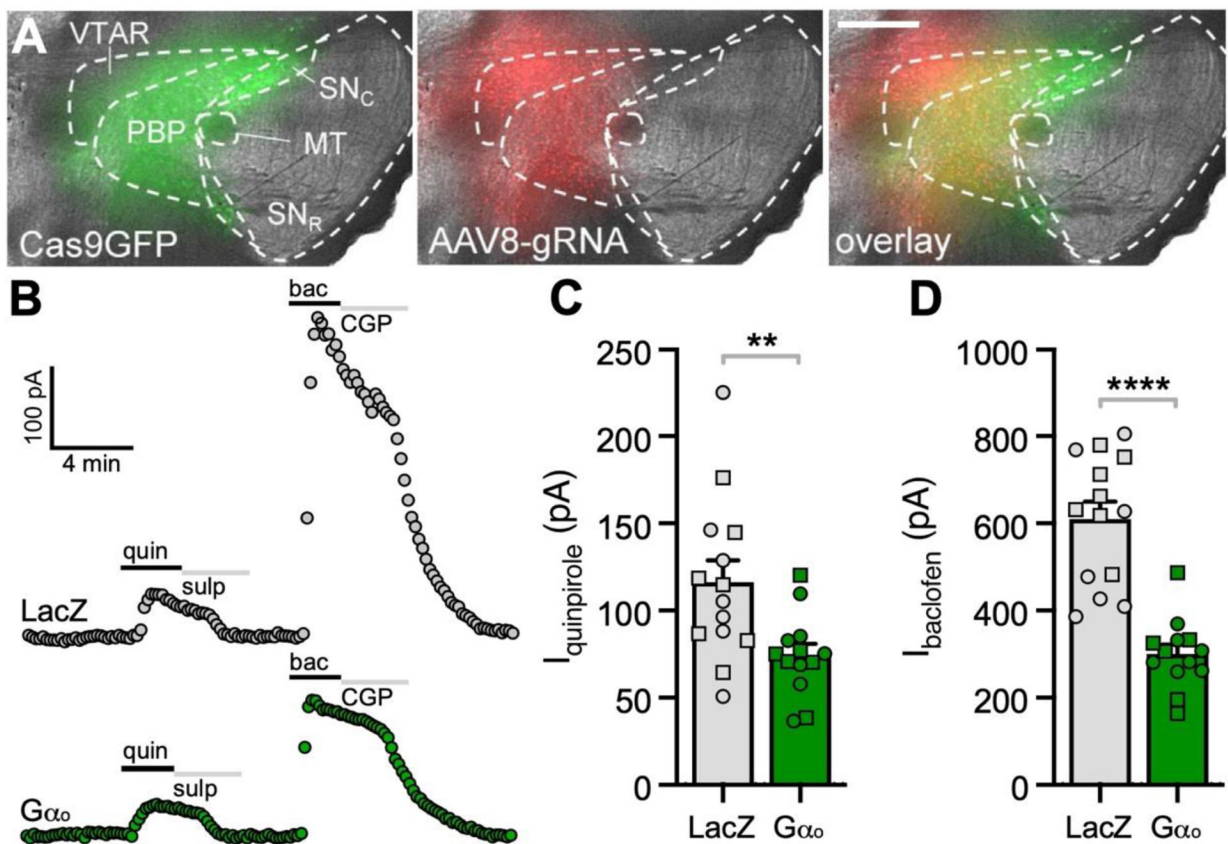


Figure 2. $G\alpha_o$ mediates D_2R - and $GABA_{\beta}R$ -dependent signaling in VTA DA neurons

A. Viral targeting in a $DATCre(+):Cas9GFP(+)$ mouse. GFP fluorescence shows the Cre-dependent expression of Cas9GFP in DA neurons of the VTA and substantia nigra pars compacta (green, left panel), and nucleus-localized mCherry fluorescence (red, middle panel) reveals the scope of viral targeting; the right panel shows the GFP/mCherry overlay. Abbreviations: MT – medial terminal nucleus of the accessory optic tract; PBP – parabrachial pigmented nucleus of the VTA; SN_C – substantia nigra pars compacta; SN_R – substantia nigra pars reticulata; VTAR – rostral part of the VTA. Scale: 400 μ m.

B. Somatodendritic currents ($V_{hold} = -60$ mV) evoked by bath application of quinpirole (quin, 20 μ M) and then baclofen (bac, 200 μ M) in VTA DA neurons from $DATCre(+):Cas9GFP(+)$ mice treated with vectors harboring LacZ control (upper trace) or $G\alpha_o$ -specific (lower trace) gRNAs. Quinpirole-induced currents were reversed by the $D_{2/3}R$ antagonist sulpiride (sulp, 5 μ M) and baclofen-induced currents were reversed by the $GABA_{\beta}R$ antagonist CGP54626 (CGP, 2 μ M).

C. Peak currents evoked by quinpirole in VTA DA neurons from $DATCre(+):Cas9GFP(+)$ mice treated with LacZ or $G\alpha_o$ gRNA-containing vector. Data points from male and female subjects are indicated in this and all following figures by squares and circles, respectively. Two-way ANOVA did not reveal a main effect of sex ($F_{1,23}=0.04$; $P=0.84$) or interaction between sex and viral treatment ($F_{1,23}=0.09$; $P=0.76$), so within-treatment data from male and female subjects were pooled and re-analyzed by unpaired t test with Welch's correction ($t_{19,61}=3.01$; $**P=0.0070$; $N=7$ mice/viral treatment and $n=13-14$ recordings/viral treatment).

D. Peak currents evoked by baclofen (after quinpirole) in VTA DA neurons from DATCre(+):Cas9GFP(+) mice treated with LacZ or $G\alpha_o$ gRNA-containing vectors. Two-way ANOVA did not reveal a main effect of sex ($F_{1,23}=1.40$; $P=0.25$) or interaction between sex and viral treatment ($F_{1,23}=1.27$; $P=0.27$), so within-treatment data from male and female subjects were pooled and re-analyzed by unpaired t test with Welch's correction ($t_{20,22}=6.85$; **** $P<0.0001$).

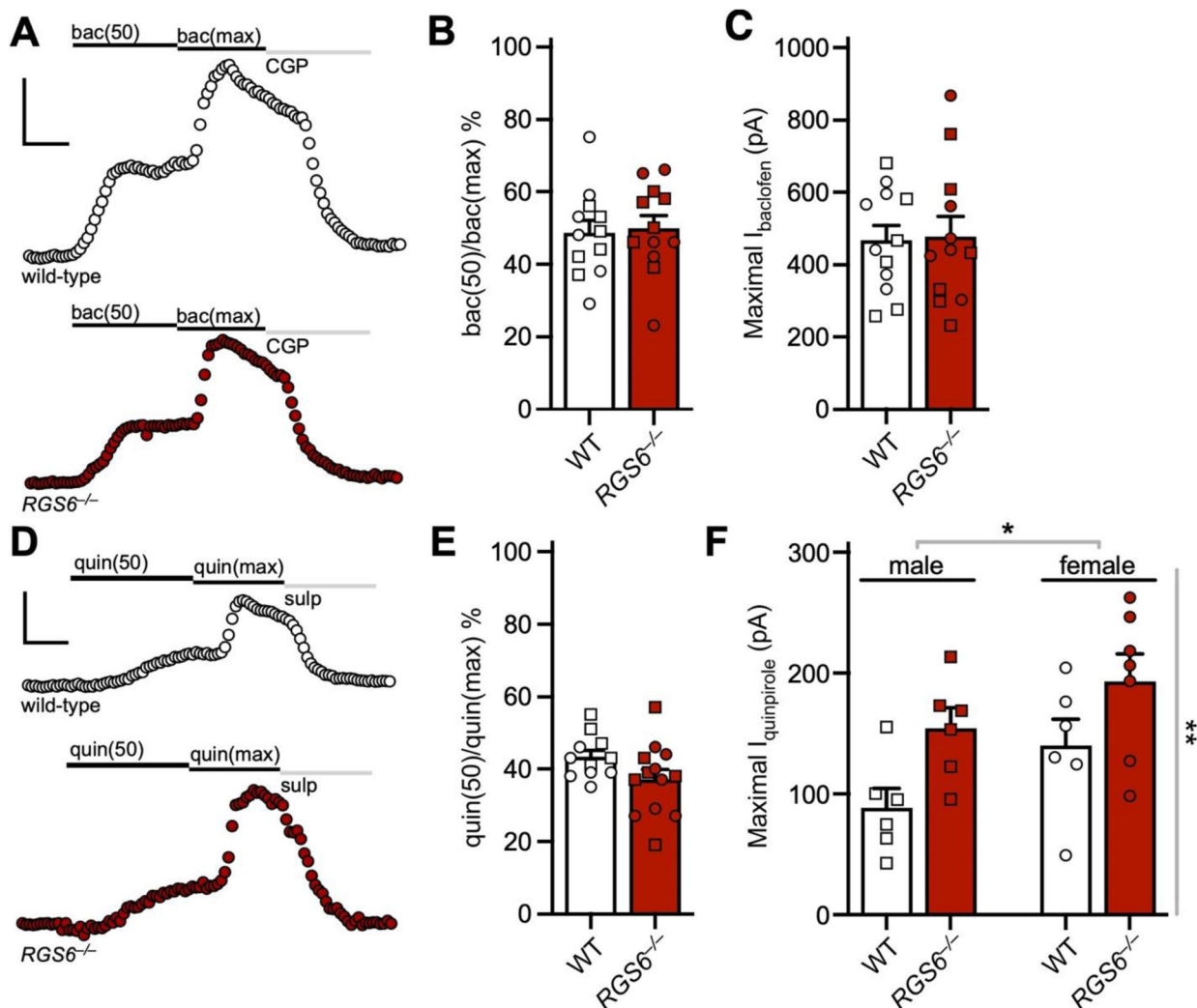


Figure 3. GABA_BR- and D₂R-dependent currents in VTA DA neurons from wild-type and *RGS6*^{-/-} mice

A. Somatodendritic currents ($V_{\text{hold}} = -60$ mV) evoked by EC₅₀ (*bac(50)*; 10 μM) and maximal (*bac(max)*; 200 μM) doses of baclofen, measured in putative VTA DA neurons from wild-type (upper) and *RGS6*^{-/-} (lower) mice. Currents were reversed by the GABA_BR antagonist CGP54626 (CGP, 2 μM).

B. Baclofen sensitivity (ratio of current evoked by EC₅₀ and maximal baclofen doses; *bac(50)/bac(max)*), expressed as a percentage) of putative DA neurons from wild-type (WT) and *RGS6*^{-/-} mice. Two-way ANOVA did not reveal a main effect of sex ($F_{1,20}=0.0003$; $P=0.99$) or interaction between sex and genotype ($F_{1,20}=0.49$; $P=0.49$), so within-genotype data from male and female subjects were pooled and re-analyzed by unpaired t test with Welch's correction ($t_{21,99}=0.25$, $P=0.80$; $N=5-6$ mice/genotype and $n=12-13$ experiments/genotype).

C. Maximal currents evoked by baclofen (200 μM) in putative DA neurons from WT and *RGS6*^{-/-} mice. Two-way ANOVA did not reveal a main effect of sex ($F_{1,20}=0.62$; $P=0.44$) or interaction between sex and genotype ($F_{1,20}=0.03$; $P=0.87$), so within-genotype data from

male and female subjects were pooled and re-analyzed by unpaired t test with Welch's correction ($t_{20,28}=0.15$; $P=0.88$).

D. Somatodendritic currents ($V_{\text{hold}} = -60$ mV) evoked by EC_{50} (quin(50); 60 nM) and maximal (quin(max); 20 μM) doses of quinpirole, measured in putative VTA DA neurons from wild-type (upper) and $RGS6^{-/-}$ (lower) mice. Currents were reversed by the $D_{2/3}R$ -selective antagonist sulpiride (sulp, 5 μM).

E. Quinpirole sensitivity (ratio of currents evoked by EC_{50} and maximal quinpirole doses; quin(50)/quin(max), expressed as a percentage) of putative DA neurons in from wild-type (WT) and $RGS6^{-/-}$ mice. Two-way ANOVA did not reveal a main effect of sex ($F_{1,21}=3.60$; $P=0.07$) or interaction between sex and genotype ($F_{1,21}=0.97$; $P=0.34$), so within-genotype data from male and female subjects were pooled and re-analyzed by unpaired t test with Welch's correction ($t_{20,12}=1.90$, $P=0.072$; $N=6$ mice/genotype and $n=11-13$ experiments/genotype).

F. Maximal currents evoked by quinpirole in putative DA neurons from WT and $RGS6^{-/-}$ mice. Two-way ANOVA revealed main effects of sex ($F_{1,21}=5.10$, $*P=0.035$) and genotype ($F_{1,21}=8.85$, $**P=0.0072$) but no interaction between sex and genotype ($F_{1,21}=0.10$, $P=0.75$; $N=3$ mice/sex and genotype and $n=6-7$ experiments/sex and genotype).

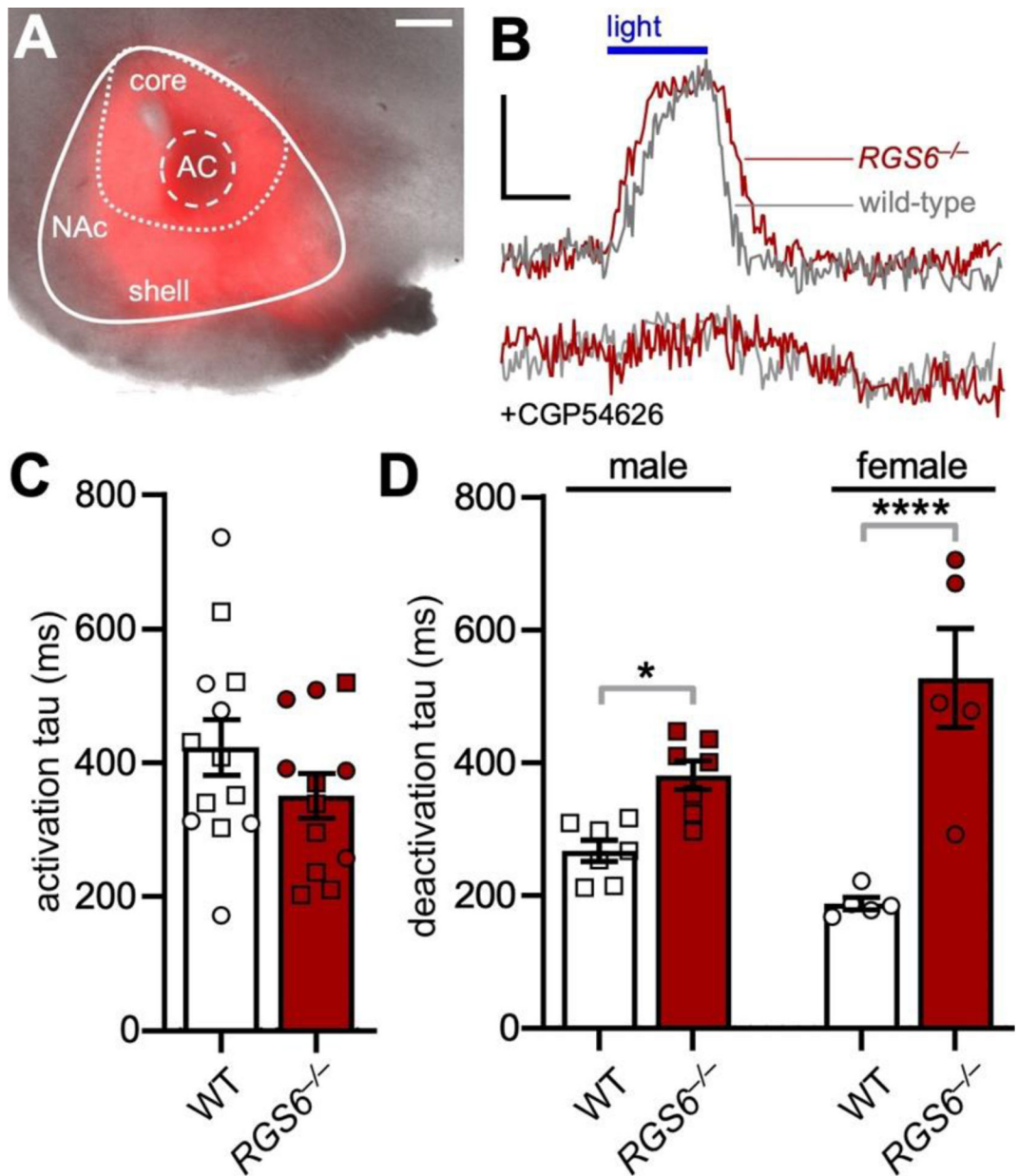


Figure 4. Optically evoked GABA_B-dependent IPSCs in VTA DA neurons from wild-type and *RGS6*^{-/-} mice

A. mCherry fluorescence in the nucleus accumbens (NAc) of an *RGS6*^{-/-} mouse treated with AAV8-CaMKII α -hChR2(H134R)-mCherry vector. Abbreviations: AC – anterior commissure. Scale: 250 μ m.

B. GABA_B-dependent inhibitory postsynaptic currents ($V_{\text{hold}} = -60$ mV) measured in putative VTA DA neurons from *RGS6*^{-/-} (red) mice and wild-type controls (gray), evoked by optical stimulation (blue bar) of hChR2-expressing NAc terminals in the VTA; the lower traces show that evoked responses were blocked by bath perfusion of the GABA_B-selective antagonist CGP54626 (2 μ M, lower trace). Scale bars: 20 pA/500 ms.

C. Activation rate (tau) of light-evoked IPSCs in putative VTA DA neurons from wild-type (WT) and *RGS6*^{-/-} mice. Two-way ANOVA did not reveal a main effect of sex ($F_{1,23}=0.37$;

$P=0.55$) or interaction between sex and genotype ($F_{1,23}=0.47$; $P=0.50$), so within-genotype data from male and female subjects were pooled and re-analyzed by unpaired t test with Welch's correction ($t_{22,18}=1.36$, $P=0.19$; $N=5-6$ mice/genotype and $n=12-13$ experiments/genotype).

D. Deactivation rate (τ) of light-evoked IPSCs in putative VTA DA neurons from WT and *RGS6*^{-/-} mice. Two-way ANOVA did not reveal a main effect of sex ($F_{1,20}=0.91$, $P=0.35$), but did detect main effect of genotype ($F_{1,20}=41.42$, $P<0.0001$) and an interaction between sex and genotype ($F_{1,20}=10.29$, $P=0.0044$). Sidak's multiple comparisons test revealed significant genotype differences in deactivation rate in putative VTA DA neurons from both male (* $P=0.042$) and female (**** $P<0.0001$) mice ($N=2-3$ mice/sex and genotype and $n=5-7$ experiments/sex and genotype).

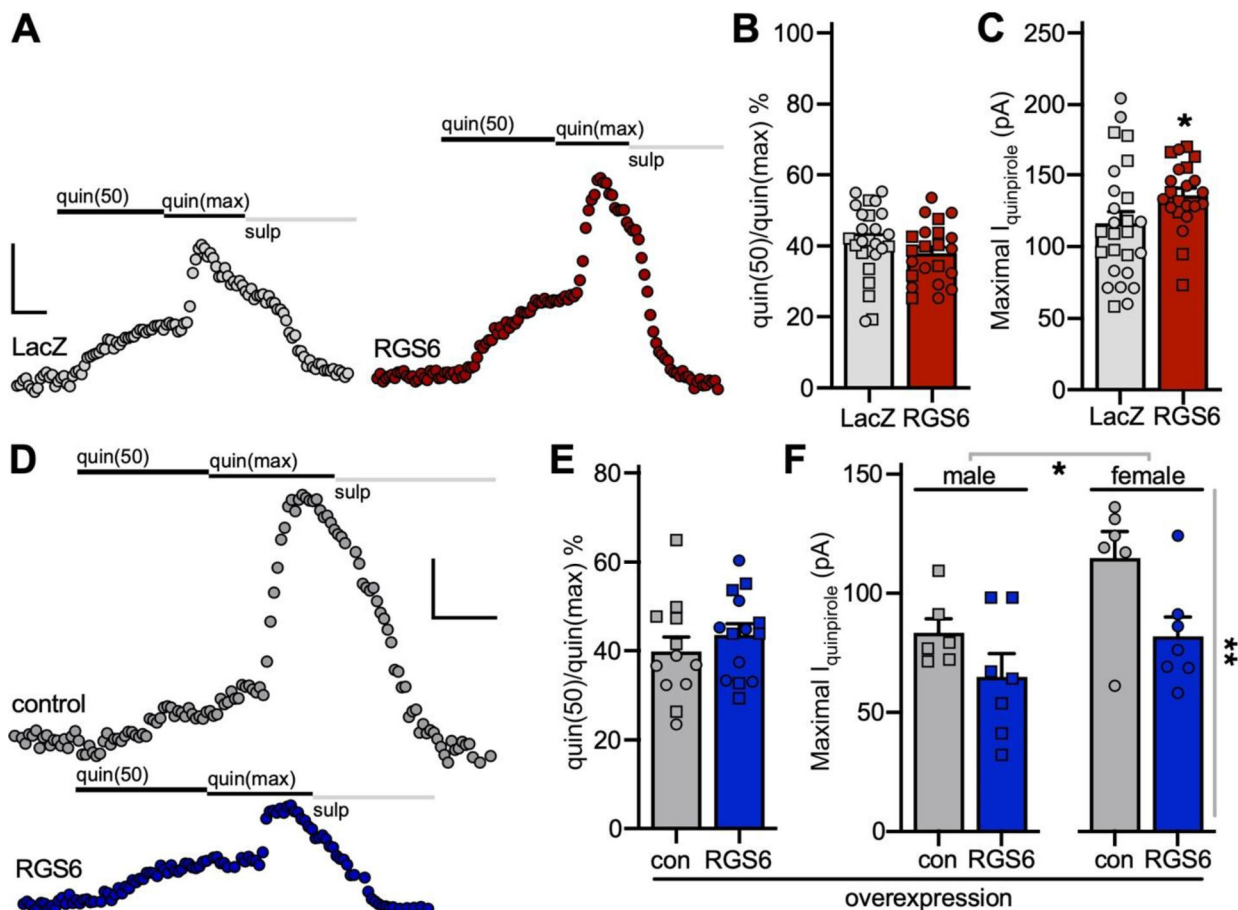


Figure 5. Impact of RGS6 ablation and overexpression on D₂R-dependent somatodendritic currents in VTA DA neurons

A. Somatodendritic currents ($V_{\text{hold}} = -60$ mV) evoked by EC₅₀ (quin(50); 60 nM) and maximal (quin(max); 20 μ M) doses of quinpirole, measured in VTA DA neurons from DATCre(+):Cas9GFP(+) mice treated with AAV8-U6-gLacZ-hSyn-NLSmCherry (LacZ) control or AAV8-U6-gRGS6-hSyn-NLSmCherry (RGS6) vector. Currents were reversed by sulpiride (sulp, 5 μ M).

B. Quinpirole sensitivity (ratio of currents evoked by EC₅₀ and maximal quinpirole doses; quin(50)/quin(max), expressed as a percentage) of VTA DA neurons from DATCre(+):Cas9GFP(+) mice treated with LacZ control or RGS6 gRNA vector. Two-way ANOVA did not reveal a main effect of sex ($F_{1,44}=0.97$; $P=0.33$) or interaction between sex and viral treatment ($F_{1,44}=1.41$; $P=0.24$), so within-viral treatment data from male and female subjects were pooled and re-analyzed by unpaired t test with Welch's correction ($t_{46.00}=1.29$; $P=0.20$; $N=16-19$ mice/viral treatment and $n=22-26$ experiments/viral treatment).

C. Maximal currents evoked by quinpirole in VTA DA neurons from DATCre(+):Cas9GFP(+) mice treated with LacZ control or RGS6 gRNA vector. Two-way ANOVA did not reveal a main effect of sex ($F_{1,44}=0.0016$; $P=0.97$) or interaction between sex and viral treatment ($F_{1,45}=0.009$; $P=0.92$), so within-viral treatment data from male and female subjects were pooled and re-analyzed by unpaired t test with Welch's correction

($t_{40,93}=2.17$; $*P=0.036$; $N=16-19$ mice/viral treatment and $n=22-26$ experiments/viral treatment). Three data points from male subjects, 1 from the LacZ gRNA and 2 from the RGS6 gRNA treatment group, were identified as outliers and excluded from final analysis.

D. Somatodendritic currents ($V_{\text{hold}}=-60$ mV) evoked by EC_{50} (quin(50), 60 nM) and maximal (quin(max), 20 μM) doses of quinpirole, measured in VTA DA neurons from DATCre(+) mice treated with AAV8-DIO-hSyn-GFP (control) or AAV8-DIO-hSyn-RGS6-IRES-GFP (RGS) vector. Currents were reversed by sulpiride (Sulp, 5 μM).

E. Quinpirole sensitivity (ratio of currents evoked by EC_{50} and maximal quinpirole doses; quin(50)/quin(max), expressed as a percentage) of VTA DA neurons from DATCre(+) mice treated with Cre-dependent control or RGS6 expression vector. Two-way ANOVA did not reveal a main effect of sex ($F_{1,22}=2.75$; $P=0.11$) or interaction between sex and viral treatment ($F_{1,22}=2.82$; $P=0.11$), so within-viral treatment data from male and female subjects were pooled and re-analyzed by unpaired t test with Welch's correction ($t_{21,46}=0.90$, $P=0.38$; $N=6-9$ mice/viral treatment and $n=12-14$ experiments/viral treatment).

F. Maximal currents evoked by quinpirole in VTA DA neurons from DATCre(+) mice treated with control or RGS6 expression vector. Two-way ANOVA revealed main effects of viral treatment ($F_{1,22}=8.10$, $**P=0.0095$) and sex ($F_{1,22}=7.19$, $*P=0.014$), but no interaction between sex and viral treatment ($F_{1,22}=0.6404$, $P=0.4321$; $N=3-6$ mice/sex and genotype and $n=6-7$ experiments/sex and genotype).

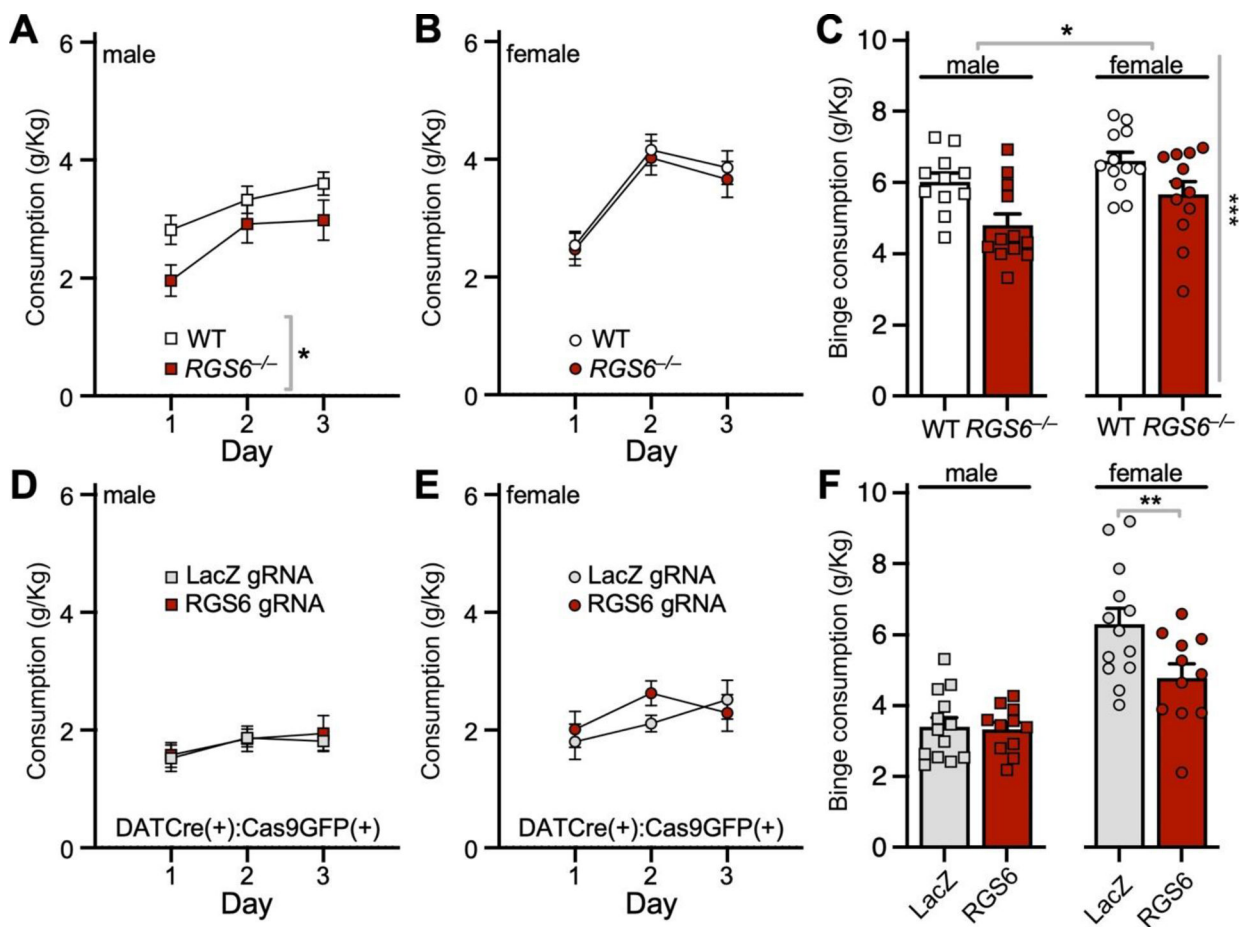


Figure 6. Impact of RGS6 ablation on binge alcohol consumption

A. Two-way repeated measures ANOVA of alcohol consumption for male WT and *RGS6*^{-/-} mice across the first 3 d of the DID test. Main effects of day ($F_{1,839, 38.63}=9.66$, $P<0.001$) and genotype ($F_{1,21}=4.53$, $*P=0.045$) were observed, but there was no interaction between day and genotype ($F_{2,42}=0.52$, $P=0.60$; $N=11-12$ mice/genotype).

B. Two-way repeated measures ANOVA of alcohol consumption for female WT and *RGS6*^{-/-} mice across the first 3 days of the DID test. A main effect of day was detected ($F_{1,969,41.34}=18.32$, $P<0.0001$; $N=11-12$ mice/genotype), but we did not detect a main effect of genotype ($F_{1,21}=0.34$, $P=0.57$) or an interaction between day and genotype ($F_{2,42}=0.028$, $P=0.97$).

C. Alcohol consumption for wild-type (WT) and *RGS6*^{-/-} mice during the 4-h binge session (day 4). Two-way ANOVA revealed main effects of sex ($F_{1,43}=5.841$, $*P=0.020$) and genotype ($F_{1,43}=12.79$, $***P=0.0009$), but no interaction between sex and genotype ($F_{1,43}=0.2097$, $P=0.6493$; $N=11-12$ mice per sex and genotype).

D. Two-way repeated measures ANOVA of alcohol consumption for male DATCre(+):Cas9GFP(+) mice treated with LacZ control or gRGS6 vector, as measured across the first 3 days of the DID test. Main effects of day ($F_{1,872,41.19}=1.60$, $P=0.21$; $N=11-13$ mice/viral treatment) or viral treatment ($F_{1,22}=0.089$, $P=0.77$) were not observed, nor was an interaction between day and viral treatment ($F_{2,44}=0.060$, $P=0.94$).

E. Two-way repeated measures ANOVA of alcohol consumption for female DATCre(+):Cas9GFP(+) mice treated with LacZ control or gRGS6 vectors, as measured across the first 3 days of the DID test. Main effects of day ($F_{1,962,43.16}=2.75$, $P=0.076$; $N=11-13$ mice/viral treatment) or viral treatment ($F_{1,22}=0.35$, $P=0.56$) were not observed, nor was an interaction between day and viral treatment ($F_{2,44}=1.23$, $P=0.3017$).

F. Alcohol consumption for DATCre(+):Cas9GFP(+) mice treated with AAV8-U6-gLacZ-hSyn-NLSmCherry (LacZ) control or AAV8-U6-gRGS6-hSyn-NLSmCherry (RGS6) vector, as measured during the day 4 binge session. Two-way ANOVA revealed main effects of viral treatment ($F_{1,44}=5.10$, $P=0.029$; $N=11-13$ mice/sex and viral treatment) and sex ($F_{1,44}=38.52$, $P<0.0001$), as well as a significant interaction between viral treatment and sex ($F_{1,44}=4.238$, $P=0.0455$). Sidak's multiple comparisons test revealed a significant difference in binge consumption between female control and RGS6 gRNA-treated mice (** $P=0.0077$); only within-sex comparisons are denoted in the interest of clarity.

Table 1.

Electrophysiological properties of VTA DA neurons

Groups	N/n	C _M (pF)	R _M (MΩ)	I _h (pA)	Activity (Hz)	Rheobase (pA)
LacZ gRNA	7/14	62 ± 2	213 ± 25	316 ± 49	1.6 ± 0.2	-19 ± 4
Gα _o gRNA	7/13	70 ± 4	177 ± 13	382 ± 56	1.6 ± 0.3	-11 ± 4
F(sex)		2.42 (P=0.13)	0.84 (P=0.37)	1.22 (P=0.28)	1.53 (P=0.23)	0.02 (P=0.88)
F(interaction)		0.71 (P=0.41)	2.84 (P=0.11)	1.67 (P=0.21)	1.65 (P=0.21)	0.35 (P=0.56)
unpaired t test		t _{19,59} =1.78	t _{19,69} =1.28	t _{24,23} =0.89	t _{18,21} =0.029	t ₂₅ =1.26
		P=0.090	P=0.22	P=0.38	P=0.98	P=0.22
wild-type	12/24	72 ± 3	200 ± 19	413 ± 38	1.7 ± 0.2	-24 ± 3
RGS6 ^{-/-}	11/25	65 ± 3	216 ± 17	433 ± 52	1.9 ± 0.2	-22 ± 4
F(sex)		1.55 (P=0.22)	0.02 (P=0.90)	1.02 (P=0.32)	0.13 (P=0.72)	0.09 (P=0.77)
F(interaction)		0.65 (P=0.42)	0.02 (P=0.89)	0.07 (P=0.79)	0.08 (P=0.78)	1.81 (P=0.19)
unpaired t test		t ₄₇ =1.85	t _{45,93} =0.64	t _{43,36} =0.32	t _{45,2} =0.67	t _{46,69} =0.37
		P=0.071	P=0.53	P=0.75	P=0.51	P=0.71
LacZ gRNA	19/26	65 ± 3	192 ± 11	343 ± 29	1.3 ± 0.1	-12 ± 3
RGS6 gRNA	16/22	68 ± 2	184 ± 11	297 ± 28	1.5 ± 0.2	-19 ± 3
F(sex)		1.92 (P=0.17)	3.21 (P=0.08)	0.007 (P=0.93)	0.32 (P=0.58)	0.06 (P=0.80)
F(interaction)		1.93 (P=0.17)	1.99 (P=0.17)	1.85 (P=0.18)	1.01 (P=0.32)	0.06 (P=0.80)
unpaired t test		t _{45,94} =0.68	t _{45,16} =0.51	t _{45,97} =1.13	t _{39,73} =0.65	t _{45,24} =1.59
		P=0.49	P=0.62	P=0.27	P=0.52	P=0.12
GFP	6/12	63 ± 3	205 ± 23	301 ± 47	1.3 ± 0.2	-15 ± 4
RGS6(GFP)	9/14	61 ± 3	200 ± 15	292 ± 43	1.6 ± 0.2	-17 ± 5
F(sex)		0.08 (P=0.79)	0.49 (P=0.49)	2.29 (P=0.14)	0.13 (P=0.72)	1.56 (P=0.23)
F(interaction)		0.74 (P=0.40)	0.48 (P=0.49)	0.62 (P=0.44)	0.83 (P=0.37)	0.12 (P=0.74)
unpaired t test		t _{23,46} =0.55	t _{19,48} =0.18	t _{23,27} =0.13	t _{23,91} =1.21	t _{21,39} =0.31
		P=0.59	P=0.86	P=0.90	P=0.24	P=0.76

Electrophysiological parameters extracted from whole-cell recordings of VTA DA neurons from DATCre(+):Cas9GFP(+) mice treated with intra-VTA control (LacZ) or Gα_o gRNAs (Fig. 1); wild-type or constitutive RGS6^{-/-} mice (Fig. 2); DATCre(+):Cas9GFP(+) mice treated with intra-VTA LacZ (control) or RGS6 gRNA vectors (Fig. 3); and DATCre(+) mice treated with intra-VTA control (GFP) or RGS6(GFP) overexpression vectors (Fig. 4). All data were analyzed first by two-way ANOVA with sex and either genotype or viral treatment as factors; results of those analyses are included in the table. No main effects of sex or interactions involving sex were detected in these analyses and thus, data from male and female subjects were pooled and re-analyzed by unpaired t test (with and without Welch's correction, as appropriate). Abbreviations: N/n - number of mice/total number of experiments; C_M - apparent cell capacitance; R_M - input/membrane resistance; I_h - hyperpolarization-activated current; activity - spontaneous firing rate during the 1-min following establishment of whole-cell access.